IX CONGRESSO BRASILEIRO DE ENGENHARIA E CIÊNCIAS TÉRMICAS
9th BRAZILIAN CONGRESS OF THERMAL ENGINEERING AND SCIENCES

Paper CIT02-0847

A NUMERICAL STUDY INTO SHOCK DISPLACEMENT EFFECTS FOR AEROELASTIC ANALYSIS IN TRANSONIC FLOW

Roberto G. A. Silva
Instituto de Aeronáutica e Espaço - IAE
Centro Técnico Aeroespacial - CTA
12228-904 - São José dos Campos - SP – Brazil
Phone: +55-12-3947-6500 / +55-12-3947-6482
rasilva@iae.cta.br

Olympio A. F. Mello
Instituto de Aeronáutica e Espaço - IAE
Centro Técnico Aeroespacial - CTA
12228-904 - São José dos Campos - SP – Brazil
Phone: +55-12-3947-6500 / +55-12-3947-6501
oamello@directnet.com.br

João L. F. Azevedo
Instituto de Aeronáutica e Espaço - IAE
Centro Técnico Aeroespacial - CTA
12228-904 - São José dos Campos - SP – Brazil
Phone: +55-12-3947-4601 / +55-12-3947-4617
azevedo@iae.cta.br

Abstract. *Approximate flutter analyses in transonic flow typically employ a linear flutter package with the inclusion of the nonlinear transonic effects, by applying corrections to the aerodynamic influence coefficient matrices. However, such analyses implicitly require that transonic aerodynamic loads are "locally" linear with respect to structural deformation about a given geometry. This linear behavior has been previously shown for the case of the solution of the transonic small disturbance equation (TDSE) in two-dimensional flow for small angle of attack variations, which allows a "linear boundary" to be established and appears to justify using approximate flutter analyses. In order to take in account the viscous effects, the present work employs a numerical Navier-Stokes code to verify the "locally" linear behavior of aerodynamic loads with respect to the variation of the static angle of attack. This study is aimed at identifying the conditions under which approximate flutter analyses based on corrections to aerodynamic influence coefficients may be used. The results show that viscous effects play a fundamental role in shock displacement over the airfoil, which prompts the re-evaluation of the previous inviscid-based linear boundaries. Thus, the locally linear behavior in transonic flow should be approached with care when applied to transonic flutter analysis.*

Keywords. *Transonic Flow, Navier-Stokes, Computational Fluid Dynamics, Linear-Non Linear Behavior*

1. Introduction

The severity of flutter at transonic speeds is linked to the presence of moving shock waves over the wing surface (Ashley, 1980) with the flutter dynamic pressure being substantially reduced for Mach numbers near unity, in a phenomenon usually termed as "transonic dip" (Whitlow, 1987). From these considerations, it is clear that accurate flutter predictions depend on the ability of computational fluid dynamic procedures to predict correct shock strength and location in a time accurate fashion.

Transonic flutter clearance relies on experience combined with costly and time-consuming wind tunnel and/or flight tests. More recently, computational aeroelasticity has allowed coupled aerodynamic /structural dynamic computations in the transonic regime. However, the computational resources needed for this coupled analysis are quite significant so its industrial application is still limited .

Approximate flutter analyses in transonic flow typically employ a linear flutter package with the inclusion of the nonlinear transonic effects, by applying corrections to the aerodynamic influence coefficient matrices (e.g. Baker & Rodden, 1999; Brink-Spalink & Bruns, 2001; Palacios et al., 2001; Silva, Mello & Azevedo, 2001). However, such analyses implicitly require that transonic aerodynamic loads are "locally" linear with respect to structural deformation about a given geometry. This linear behavior has been shown Dowell (1995) in two-dimensional flow for small dynamic angles of attack, which allows a "linear boundary" to be established and appears to justify using the approximate flutter analyses.

Dowell's investigation was performed using a TSD code, which does not include viscous effects. An investigation into local linearity in unsteady transonic 3-D flow has been conducted by Silva et al (2002). Their results indicate that the linear boundaries may be more restrictive in 3-D flow. In order to clarify the role of the viscous effects in the non linearities which were identified by Silva et al., the present work employs a 2-D Navier-Stokes code to investigate the quasi-static behavior of the shock waves with respect to angle of attack in viscous flow. Simulations are conducted in steady flow for a set of increasing angles of attack, from which the shock displacement with respect to angle of attack may be evaluated.

2. Numerical Method

The Navier-Stokes solver used in the present work is a version of a code developed by Menezes, (1994). The thin layer Reynolds-averaged, 2-D Navier-Stokes equations based on an arbitrary curvilinear coordinate system can be written in non-dimensional form as (Azevedo, 1993):

$$\overline{Q}_\tau + \overline{E}_\xi + \overline{F}_\eta = \mathrm{Re}_c^{-1}\,\overline{S}_\eta \tag{1}$$

where $\overline{Q}$ is the vector of unknown flow properties; $\overline{E}$ and $\overline{F}$ are the inviscid flux vectors; $\overline{S}$ is the thin layer viscous flux vector and $\mathrm{Re}_c = \rho_\infty a_\infty c/\mu_\infty$ is the Reynolds number, based on the airfoil chord ρ_∞, a_∞ and μ_∞ are the free stream density, speed of the sound and viscosity, respectively.

For the numerical solution of the system of Eqns. (1), an implicit approximate factorization algorithm is employed. Originally this algorithm was idealized by Beam and Warming (1976) for Cartesian coordinates and later it was generalized for a curvilinear coordinate system and applied for the numerical solution of the thin layer Navier-Stokes equations by Steger (1978). The time derivative, $\overline{Q}_\tau$, of equation (1) is approximated using the implicit Euler method, a first order method, and all spatial derivatives are approximated by standard second-order central differences .

With the above described time and space discretizations, the application of the approximate factorization leads to:

$$L_\xi L_\eta \Delta_t \overline{Q}^n = R_\xi + R_\eta \tag{2}$$

with:

$$L_\xi = \left(I + \Delta t\delta_\xi A^n - \Delta t\varepsilon_I J^{-1}\nabla_\xi\Delta_\xi J\right) \tag{3}$$

$$L_\eta = \left(I + \Delta t\delta_\eta B^n - \Delta t\varepsilon_I J^{-1}\nabla_\eta\Delta_\eta J\right) - \Delta t\,\mathrm{Re}^{-1}\,\overline{\delta}_\eta J^{-1}M^n J \tag{4}$$

$$R_\xi = \left(\Delta t\delta_\xi \overline{E}^n - \Delta t\varepsilon_E J^{-1}\left(\nabla_\xi\Delta_\xi\right)^2 J\overline{Q}^n\right) \tag{5}$$

$$R_\eta = \Delta t\left(\delta_\eta \overline{F}^n - \mathrm{Re}^{-1}\,\overline{\delta}_\eta \overline{S}^n\right) - \Delta t\varepsilon_E J^{-1}\left(\nabla_\eta\Delta_\eta\right)^2 J\overline{Q}^n \tag{6}$$

In the above equations, δ_ξ and δ_η are standard second-order central differences, Δ_ξ, Δ_η and ∇_ξ, ∇_η are first order backward and forward difference operators, respectively, and $\overline{\delta}_\eta$ is a half-point second-order difference operator.

The numeric instabilities are controlled explicitly by adding linear artificial dissipation terms. These terms are the second term of equations (5) and (6) and second term of the LHS in equations (3) and (4). The ε_E and ε_I coefficients are constants of order 1.0. The definitions of the Jacobian matrices A, B and M_η and details of the implementation procedure are presented by Azevedo (1993) and Menezes (1994). In order to accelerate the convergence of the algorithm, a variable time step is employed along the mesh, respecting the constant CFL condition (Menezes, 1994).

A Baldwin-Lomax algebraic turbulence model is used, which allows the computation of the instantaneous turbulent viscosity field. The detailed implementation is presented in Menezes (1994) for curvilinear coordinates and two dimensions. The boundary conditions are based in a set of six types of boundaries such as plane wall, far field, symmetry line, wake, subsonic or supersonic entrance and exit. In two dimensions, just four variables are necessary in each of the boundaries. Details of the boundary condition implementation can be found in Azevedo (1993) and Menezes (1994).

3. Results

The computational results of the Navier-Stokes simulation for a NACA 0012 airfoil for zero angle of attack were validated by comparison with experimental results from the work of McDevitt & Okuno, (1985) and Thibert et al, (1979) and with the numerical results presented in the work of Holst et al (1989), for set of different Mach and Reynolds numbers, as presented in the work of Menezes (1994). A good agreement with experiment has been observed for both laminar and turbulent cases. With angle of attack, the computational results were validated comparing with the experimental results presented in Harris (1981), and with the numerical results of the works of King (1987), and

Coakley (1987). Table 1 presents the Mach numbers with the corresponding angle of attacks for the above mentioned validation cases.

Table 1. Validation test cases presented in Menezes (1994).

Mach	Re_c ($\times 10^{-6}$)	α (deg)
0.800	12.0	0.00
0.800	4.09	0.00
0.830	4.09	0.00
0.700	9.00	1.49
0.550	9.00	8.34
0.799	9.00	2.26

For the present study, a variation in angle of attack is investigated, in order to evaluate the shock displacement in transonic regime. One should note that, the simulations are performed for a number of steady state situations of the airfoils for different angles of attack. Table 2 presents the test cases employed for this evaluation. The Reynolds number is $Re_c = 12.0 \times 10^6$, and the Mach number is 0.8. In this situation a strong shock wave appears in the upper and lower surfaces of the airfoil, when $\alpha = 0^0$. For angles of attack greater than zero, the lower surface shock is weakened and eventually disappears.

Table 2. Test cases for angle of attack evaluation (Mach = 0.8 and Re = 12.0 10^6).

Case	1	2	3	4	5	6	7	8	9	10
Alpha	1.0	1.5	2.0	2.5	3.0	3.5	4.5	5.5	6.5	8.0

The computational grid used for all cases had 95 by 65 algebraically generated mesh points in the ξ (tangential) and η (normal) directions, respectively. A close-up view of the grid is shown in Figure 1, where one may observe the η direction stretch, which is adequate for thin layer Navier-Stokes computations.

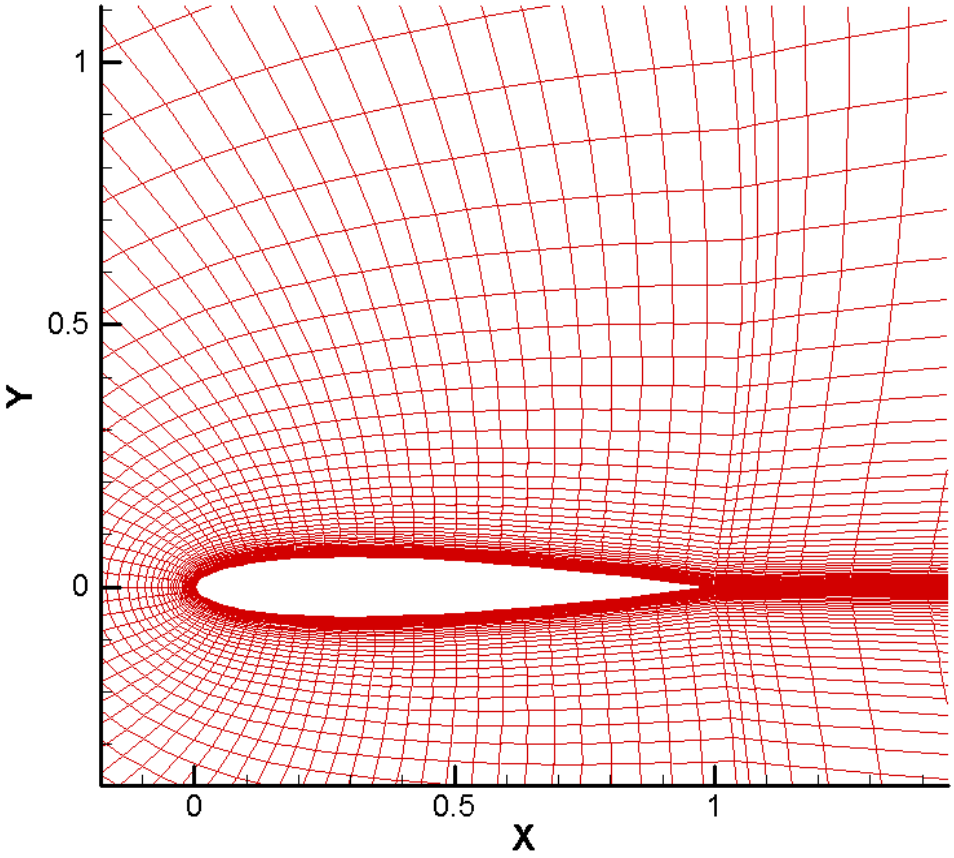

Figure 1. Mesh around a NACA 0012 airfoil.

The artificial dissipation coefficients for all test cases were set as $\varepsilon_E = 5.0$ and $\varepsilon_I = 4.0 \times \varepsilon_E$ where the subscripts E and I refer to the explicit and implicit dissipation coefficients respectively. These values were frozen in order to have

the same artificial dissipation in all the cases. A constant CFL number was chosen as 1.0, that is, a variable time step size is used for time marching. The variable step size is efficient to accelerate the convergence to the desired steady state solution. The results for the test cases listed in Table 2 are presented in Figures 2 and 3 as the differential pressure distribution ΔC_p along the non-dimensional airfoil chord x/c. In Fig. 2, the pressure differential distributions are shown for the first three angles of attack (1.0^o , 1.5^o and 2.0^o), while in Fig. 3 the pressure differentials are shown for all the angle of attack cases investigated.

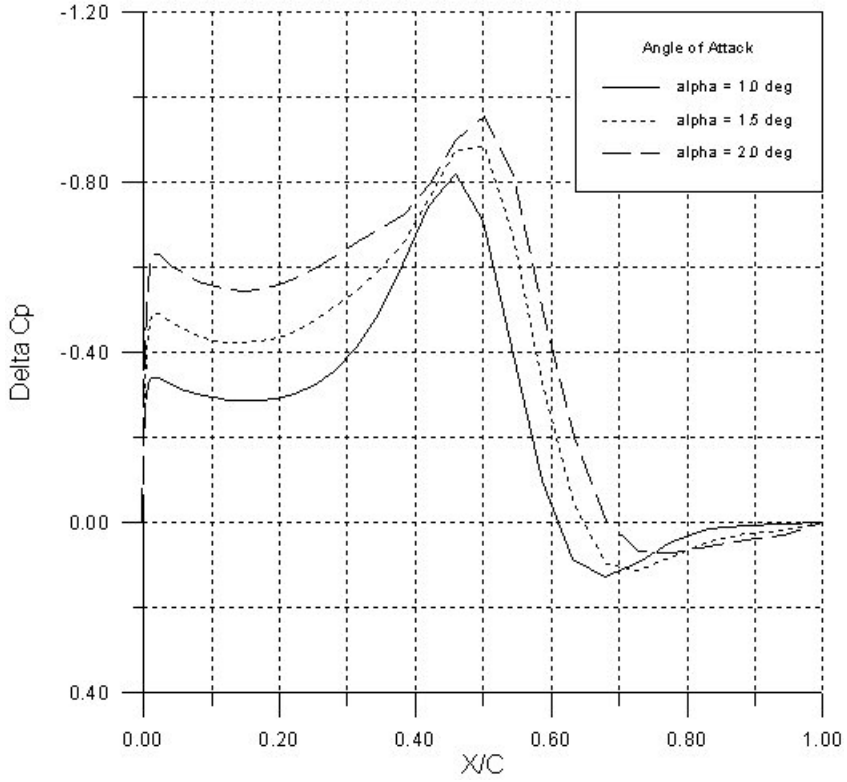

Figure 2. – Pressure differential distribution over airfoil surface for smaller angles of attack

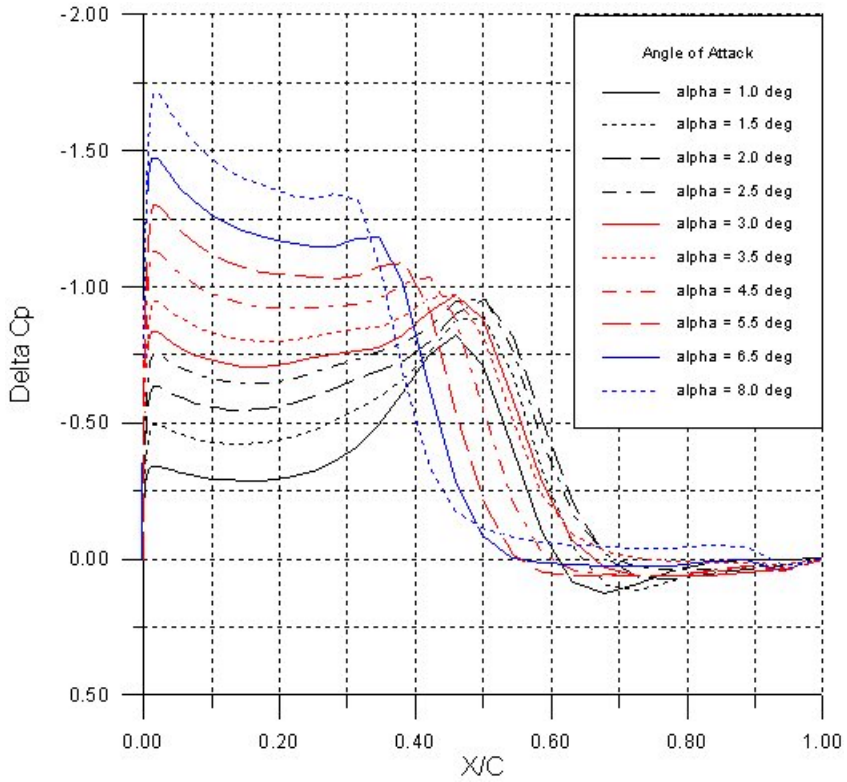

Figure 3. – Pressure differential distribution over airfoil surface for all angles of attack.

One feature to be noted is the aft movement of the chordwise shock position until 2.0°. Therefore, for small angles, the behavior is consistent with the one presented by Dowell et al. (1995) where TSDE simulations showed that, for small angles, there was an aft displacement in the shock position and an increase in shock strength with angle of attack, as may be observed in Fig. 2. However, for larger values of angle of attack, the shock position starts to move forward (towards the leading edge), as may be seen in Fig. 3. However, the shock strength keeps increasing with the angle of attack, regardless of the angle of attack, at least in the range of angles of attack investigated.

In order to understand these phenomena, a useful approach is to analyze the instantaneous viscous turbulence field μ_t and the pressure field distribution as isobaric lines as shown in Figs. 4. to 7. The viscous turbulence fields indicate that the shock wave-boundary layer interaction results in significant thickening of the turbulent boundary layer. For larger angles of attack, shock position moves forward, in the opposite direction when compared to the low angle of attack cases. In Figs. 6. and 7, the pressure and viscous turbulence fields are shown for higher angles. It is seen that the shock wave-boundary layer interaction at higher angles of attack leads to boundary layer separation, which seems to "push" the shock forward. This shock-induced separation is further illustrated by Figs. 8 and 9, where streamtraces are shown for angles of attack 6.5 and 8 deg., respectively, showing a clearly separated region after the shock.

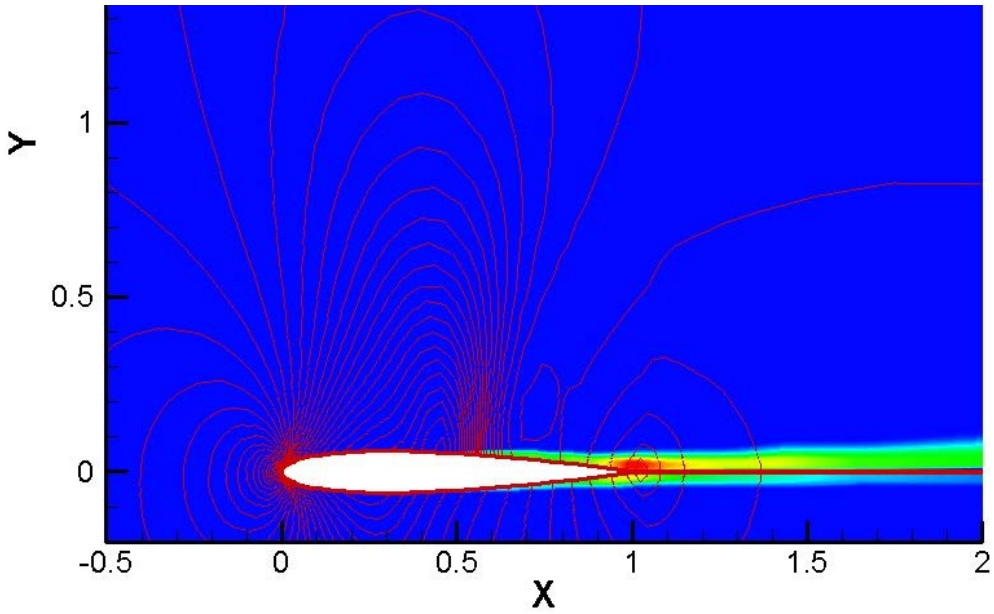

Figure 4. Instantaneous viscous turbulence field μ_t and the pressure field over a 0012 NACA airfoil, for 1 deg. angle of attack

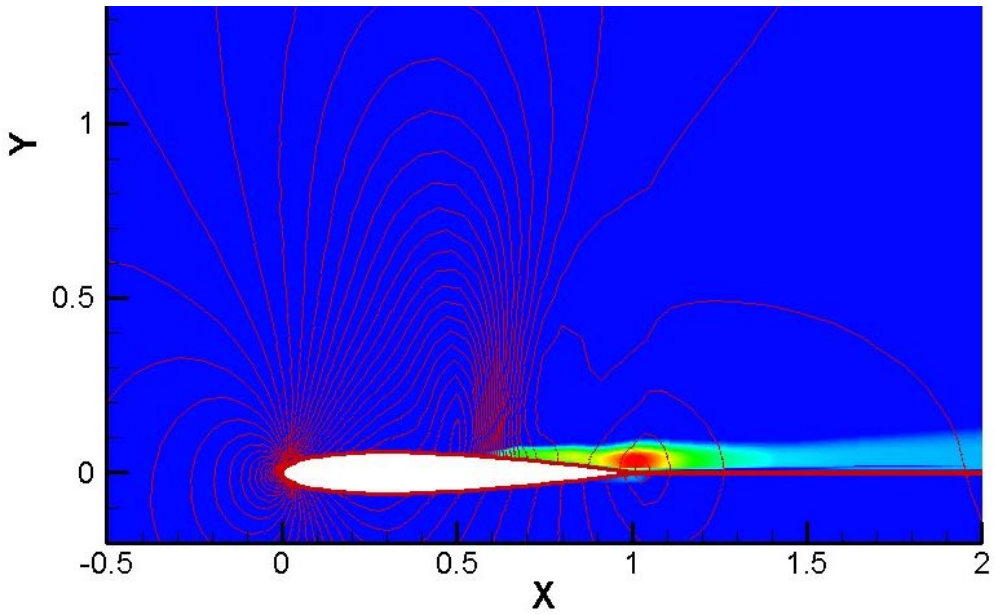

Figure 5. Instantaneous viscous turbulence field μ_t and the pressure field over a 0012 NACA airfoil, for 2 deg. angle of attack

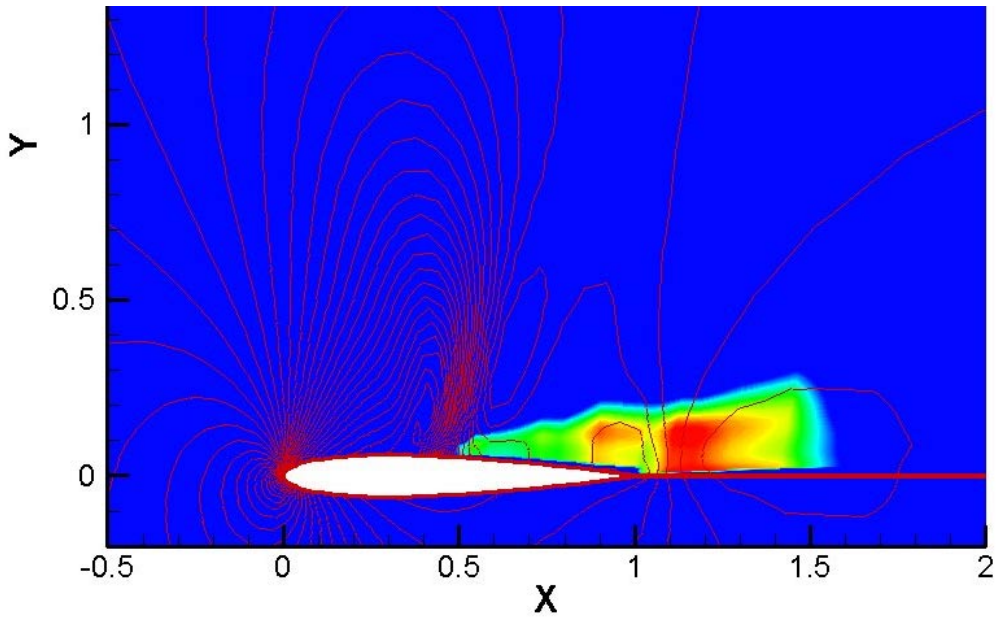

Figure 6. Instantaneous viscous turbulence field μ_t and the pressure field over a 0012 NACA airfoil, for 6.5 deg. angle of attack.

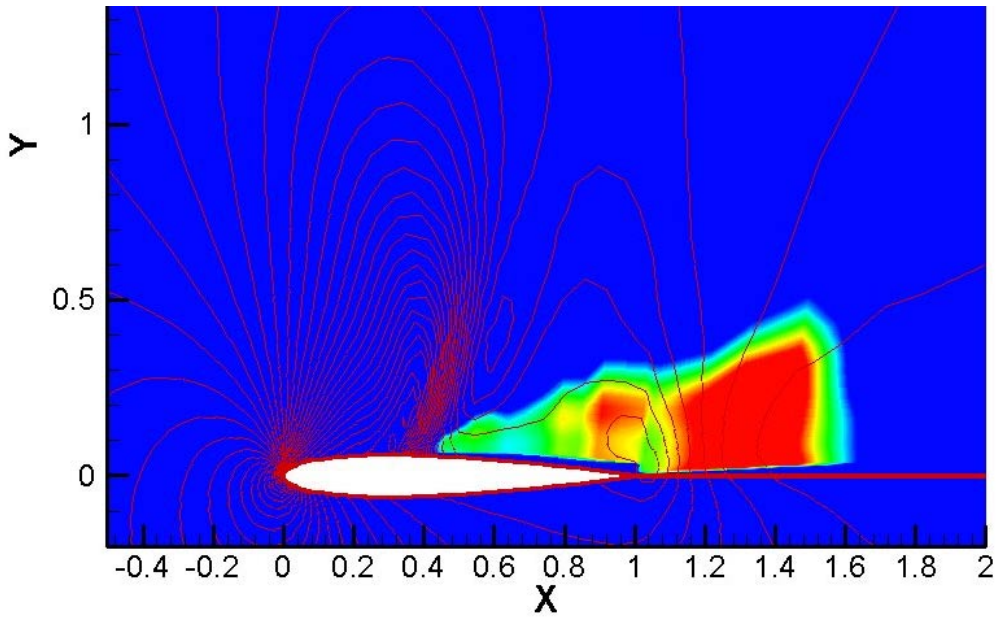

Figure 7. Instantaneous viscous turbulence field μ_t and the pressure field over a 0012 NACA airfoil, for 8 deg. angle of attack.

Even though the present investigation was limited in scope, viscous effects have been shown to play a fundamental role in shock displacement over the airfoil. Therefore, the inviscid-based studies presented by Dowell et al. (1995) should be carefully re-examined when trying to assume a locally linear behavior in transonic flow. Clearly, the same non-linear simulations shall not be used to obtain aerodynamic coefficient corrections for all angles of attack. Additionally, transonic analysis shall be conducted at a range of static angles of attack according to possible flight conditions. The increased amount of computations strengthens the case for approximate methods in transonic flow. However, further investigation is needed to establish local linearity with dynamic angle of attack around a given static angle of attack.

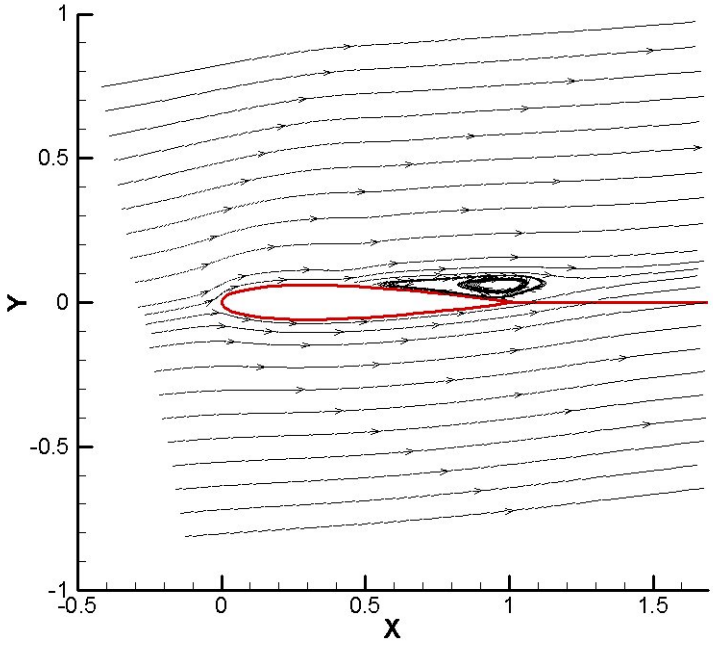

Figure 8. Streamtraces over a 0012 NACA airfoil at 6.5 deg. angle of attack.

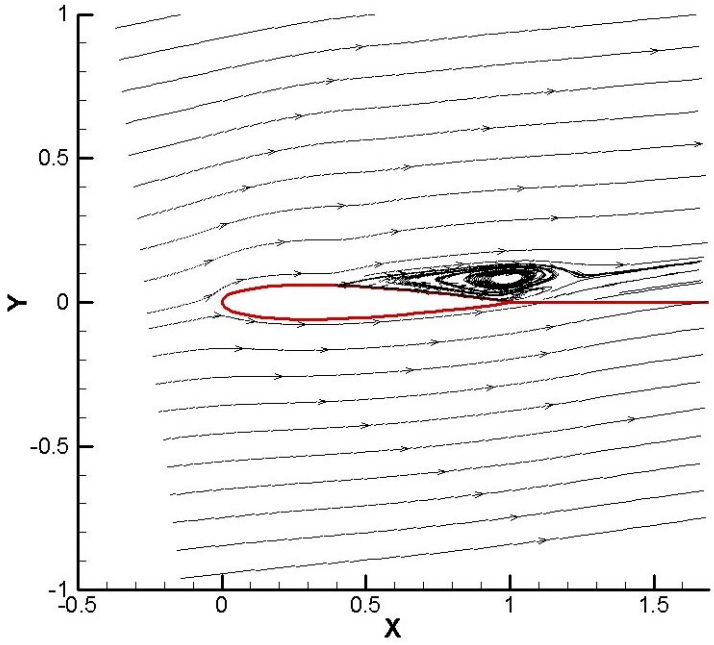

Figure 9. Streamtraces over a 0012 NACA airfoil at 8 deg. angle of attack.

4. Conclusion

The present results show that the displacement of the shock wave over the airfoil depends on the angle of attack. For small angles of attack, the shock wave moves downstream, towards the trailing edge. A change in this direction is noted when the angle of attack reaches higher values and the shock starts to move upstream. One explanation for this phenomenon is that the shock-induced separation for higher angles “pushes” the shock forward. Another interesting feature to be noted is the shock curvature, more evident at the higher angles. This behavior can be explained as a induced shock foot displacement caused by the boundary layer thickening and separation. As the angle of attack is increased beyond separation, the shock strength continues to increase. The reason for this increase and for the augmented shock curvature is associated to the "potential" field behavior; although one may argue that a thickened "equivalent inviscid body" would seem to reinforce this behavior.

Since viscous effects have been shown to play a fundamental role in shock displacement over the airfoil, the locally linear behavior in transonic flow should be approached with care. Clearly, the same non-linear simulations shall not be used to obtain aerodynamic coefficient corrections for all angles of attack. Additionally, transonic analysis shall be conducted at a range of static angles of attack according to possible flight conditions. The increased amount of

computations strengthens the case for approximate methods in transonic flow. However, further investigation is needed to establish local linearity with dynamic angle of attack around a given static angle of attack. Further studies must be performed, such as a dynamic angle of attack at a given reduced frequency in order to evaluate the phase shift due to the shock motion, which is an important aspect to be considered in the unsteady transonic aerodynamic loading.

5. Acknowledgements

The second and third authors were supported by the Conselho Nacional de Desenvolvimento Científico e Tecnológico (CNPq), Brazil, under the Integrated Project Research Grant no. 522.413/96-0.

6. References

Ashley, H., "Role of Shocks in the 'Sub-Transonic' Flutter Phenomenon," Journal of Aircraft, Vol. 17, No. 3, March 1980, pp. 187.

Azevedo, J. L. F., "Introduction to computational Fluid Dynamics", Notes for Short Course, 16th National Congress of Applied and Computational Mathematics – CNMAC 93, Uberlândia, Brasil, 1993 (in Portuguese; original title is: Introdução à Mecânica dos Fluidos Computacional").

Baker, M. L., and Rodden, W. P., "Improving the Convergence of the Doublet-Lattice Method Through Tip Corrections", CEAS/AIAA/ICASE/NASA Langley International Forum on Aeroelasticity and Structural Dynamics, Williamsburg, Virginia, USA, 1999.

Beam, R. M., and Warming, R. F., "An Implicit Finite-Difference Algorithm for Hyperbolic Systems in Conservation Law Form", Journal of Computational Physics, Vol. 22, Sept. 1976, pp. 87-110.

Brink-Spalink, J., and Bruns, J. M., "Correction of Unsteady Aerodynamic Influence Coefficients Using Experimental or CFD Data", Proc. of the CEAS/AIAA International Forum on Aeroelasticity and Structural Dynamics, Madri, Spain, June 2001, pp. 175-182.

Dowell, E. H. (editor), Crawley, E. F., Curtiss, H. C., Jr., Peters, D. A., Scanlan, R. H., and Sisto, F., A Modern Course in Aeroelasticity, 3rd edition, Kluwer, Dordrecht, Netherlands, 1995, pp. 472-487.

Landahl, M. T., Unsteady Transonic Flow, Pergamon Press, New York, 1951.

Menezes, J., C., L., "Numerical Analysis of Transonic Turbulent Flows About Airfoils", Master Dissertation, Instituto Tecnológico de Aeronáutica, São José dos Campos, Brasil, 1994, (in Portuguese; original title is "Análise Numérica de Escoamentos Transônicos Turbulentos em Torno de Aerofólios").

Palacios, R., Climent, H., Karlsson, A., and Winzell, B., "Assessment of Strategies for Correcting Linear Unsteady Aerodynamics Using CFD or Test Results", Proc. of the CEAS/AIAA International Forum on Aeroelasticity and Structural Dynamics, Madri, Spain, June 2001, pp. 195-210.

Silva, R. G. A., Mello, O. A. F., and Azevedo, J. L. F "A Navier-Stokes Based Study into Linearity in Transonic Flow fort Flutter Analysis, Proc. of the 32nd AIAA Fluid Dynamics Conference, St. Louis, USA, June 2002, AIAA Paper 2002-2971.

Silva, R. G. A., Mello, O. A. F., and Azevedo, J. L. F., "Transonic Flutter Calculations Based on Assumed Mode Shapes Corrections", Proc. of the CEAS/AIAA International Forum on Aeroelasticity and Structural Dynamics, Madrid, Spain, June 2001, pp. 183-194.

Steger, J. L., "Implicit Finite-Difference Simulation of Flow about Arbitrary Two-Dimensional Geometries", AIAA Journal, Vol. 19, No 2, Feb. 1978, pp. 679-686.

Whitlow, W., Jr., "Computational Unsteady Aerodynamics for Aeroelastic Analysis," NASA TM-100523, Dec., 1987.